Wave: Jurnal Ilmiah Teknologi Maritim
(Journal of Maritime Technology)

Vol.20 No.01, June 2026: page: 47-55
p - ISSN: 1978-886X
e - ISSN: 2614-641X

The Analysis of Ship Stability of Ferry Ro-Ro Based on Loadcase Changes

Nurhasanah* dan Egi Yuliora
Department of Naval Architecture, Politeknik Negeri Bengkalis, Riau, Indonesia

Article Info

Article history:
Received February 13, 2026
Revised April 08, 2026
Accepted April 15, 2026

Keywords:
Ferry roro
Stability
Service Speed
Monohull
Loadcase Criteria

ABSTRACT

The design of Ro-Ro ferries with low payload capacities requires a more detailed analysis, as it significantly influences vessel comfort during navigation. This study presents a case study of ferries operating on the short Bengkalis – Sungai Pakning route as an alternative solution, addressing the frequent fluctuations in passenger and vehicle demand. Consequently, during peak periods, the existing Ro-Ro capacity becomes insufficient, leading to extensive queues. Conversely, during low-demand periods, the current vessels become economically inefficient, as they often delay departure until reaching full capacity to prevent operational losses. The proposed solution involves a comparative analysis of three ship models with varying load capacities to identify the optimal configuration in terms of stability and speed performance. Utilizing an analytical modeling approach, the results indicate that Model-1 exhibits superior stability performance, characterized by principal dimensions of L = 42.3 m, B = 11.8 m, H = 3.1 m, T = 2.03 m, and a payload of 78.25 tons.

****Corresponding Author:***
Nurhasanah
Department of Naval Architecture
Politeknik Negeri Bengkalis
Riau, Indonesia
Email: nurhasanah@polbeng.ac.id

INTRODUCTION

The Bengkalis–Sungai Pakning Ro-ro ferries route is one of the routes characterized by inconsistent cargo loads. This inconsistency is evident during certain periods, such as long holidays (school holidays, Eid al-Fitr, and Christmas and New Year), when the number of vehicles results in excessively long queues, and the available ferry fleet is unable to adequately serve the demand to reduce waiting times. However, on regular days, the number of vehicles is low, and there is often an imbalance in the queue lengths between the two ports (Bengkalis and Sungai Pakning), making the operation of the existing fleet uneconomical and potentially resulting in losses if the vessels sail without full loads. The ship design process should begin with the conceptual design stage, which includes determining the hull form based on the required dimensions and capacity. The design process is an iterative series of activities carried out to produce a design that meets the desired objectives (Szymo, 2024).

In the process of designing and constructing a new vessel, several design stages are involved, namely conceptual design, preliminary design, contract design, and detailed design (Dewanto & Nasirudin, 2023). In the subsequent naval architectural design phase, the vessel's principal dimensions were derived using linear regression analysis, a robust statistical approach employed to model the correlations between fundamental design parameters (Awwalin et al., 2022). One reference states that an investigation was conducted by varying a total of four V-shaped monohull models derived from high-built designs as the main subjects, with the aim of comparing several hull form designs at the same displacement in order to achieve better performance in terms of stability, resistance, and seakeeping criteria (Projektovanja et al., 2022). This research aims to obtain a Ro-Ro ferry design characterized by superior stability characteristics in full compliance with the IMO stability standards.

In addition, modern approaches to ship design are also implemented in practice by utilizing appropriate platforms and software, introducing parametric design into the ship design process (Ariesta et al., 2021) . This enables the exploration of a very broad design space prior to decision making. These approaches are often interconnected with modular ship design, in which the main components of the vessel—such as the hull, machinery, equipment, and navigation bridge—are considered as modules with associated functionality, connectivity, as well as spatial and weight requirements (Skoupas et al., 2019).

METHOD

The determination of the ship's payload was obtained by conducting field surveys to observe vessel queues at 30-minute intervals. The 30-minute interval was established based on the results of a questionnaire distributed to users of the Ro-Ro ferry service, with a minimum target of 300 respondents by an online link https://forms.gle/qeuKDrHY3akRLkTp8.

Subsequently, after determining the number of vehicles, a layout of vehicle arrangements on the vehicle deck was developed for three ship models. Several ship models are required due to the varying queue lengths. Once the layouts are established, hull models are then created for stability and resistance analyses in order to identify the ship model with the best stability performance.

In analyzing the stability of Ro-Ro ferries, the calculations focus on the vessel's ability to return to an upright position after being inclined by external forces. Due to the characteristic of expansive vehicle decks in Ro-Ro vessels, both static and dynamic stability aspects are paramount. The following are the fundamental equations employed in the stability calculations for steel ships (Rawson, K.J; Tupper, 2001).

a. Initial of metacentric height (GM)
The GM value is the primary indicator of a vessel's initial stability. The positive GM ensures that the ship possesses a restorative moment at small angles of heel.

$$GM = KB + BM - KG \quad (1)$$

KB : Vertical center of buoyancy
The distance from the keel to the center of the displaced volume. For preliminary hull forms, it is often approximated as a function of the draft (T).
BM : Metacentric radius $BM = \frac{I}{\nabla}$
Where I denotes the transverse moment of inertia of the waterplane area and ∇ represents the volume of displacement
KG : Vertical center of gravity
The height of the ship's total weight center above the keel, derived from the comprehensive weight distribution of the vessel.

b. The righting Lever (GZ)
The GZ lever determines the magnitude of the righting moment available to return the ship to an upright position. For larger angles of inclination, the GZ value is derived using the Cross Curves of Stability (KN).

$$GZ = KN - KG \sin\theta \quad (2)$$

In Ro-Ro ferry design, the GZ curve must be analyzed extensively to ensure the vessel can withstand the dynamic forces associated with heavy vehicle loads and potential shifting of cargo.

c. Free Surface Effect
Ro-Ro ferries are particularly susceptible to the Free Surface Effect due to their wide vehicle decks and large tank configurations. The presence of unbound liquids causes a virtual rise in the center of gravity (GG′), thereby reducing the effective GM.

$$GG' = \frac{i \, x \, \rho_c}{W} \quad (3)$$

i : The second moment of area of the liquid surface
ρc : The density of the liquid within the compartment.
W : The total displacement of the vessel.

The corrected metacentric height is expressed as:
$$GM_{fluid} = GM_{solid} - GG' \quad (4)$$

RESULTS AND DISCUSSION

The initial stage in obtaining the principal ship data is to create a layout by arranging vehicles according to the predetermined number based on the payload capacity previously obtained from the survey results. The arrangement of vehicles on the ship's deck refers to the applicable regulations, which stipulate that the minimum distance between the sides of adjacent vehicles is 60 cm, and the minimum distance between the front and rear sides is 30 cm (Perhubungan, 2016).

The payload for Model-1, Model-2, and Model-3 are presented in Table 1.

Table 1. The payloads every models

No	Name of Model	Number of Vehicles
1	Model-1	15 units of motorcycles, 10 units of passenger cars, 1 unit of bus, and 1 unit of heavy goods vehicle.
2	Model-2	11 units of motorcycles, 6 units of passenger cars, and 1 unit of heavy goods vehicle.
3	Model-3	11 units of motorcycles, 6 units of passenger cars, and 1 unit of bus.

Vehicles are classified into several categories, ranging from Category I to Category IX, and these categories are regulated to determine the volumetric weight and payload carried (Ministry of Transportation Regulation No. PM 63 of 2013, 2012). In the case of the Bengkalis–Sungai Pakning ferry, the number of vehicles every 30 minutes was obtained through field surveys, resulting in the average queue as presented in Table 1.

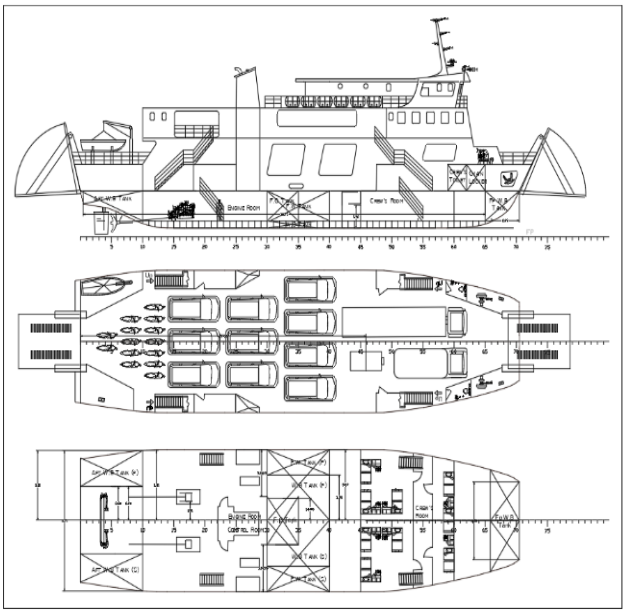

Figure 1. Model-1

Figure 1 shows the vehicle arrangement layout for Model-1 with a payload of 78,25 tons. The number of the vehicles is 15 units of motorcycles, 10 units of passenger cars, 1 unit of bus, and 1 unit of heavy goods vehicle.

Figure 2 shows the vehicle arrangement layout for Model-2 with a payload of 59,45 tons. The number of the vehicles is 11 units of motorcycles, 6 units of passenger cars and 1 unit of heavy goods vehicle.

Figure 3 shows the vehicle arrangement layout for Model-3 with a payload of 24,45 tons. The number of the vehicles is 11 units of motorcycles, 6 units of passenger cars and 1 unit of bus. After designing the vehicle layout, the next step is to create a 3D ship model using Maxsurf software.

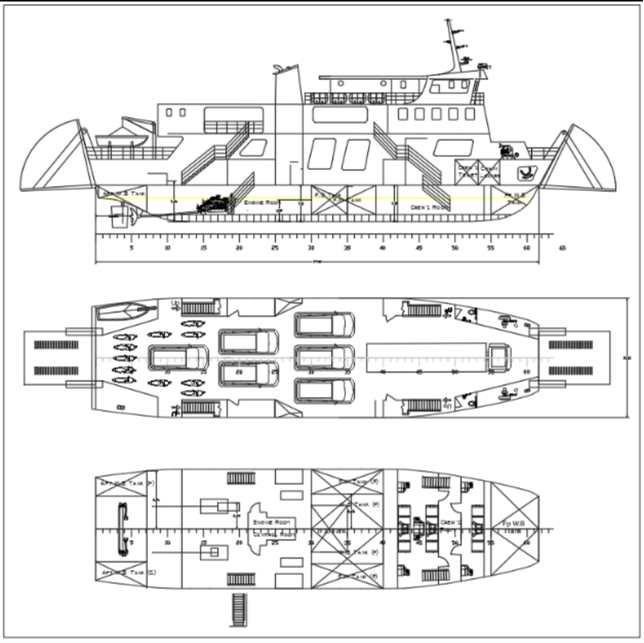

Figure 2. Model-2

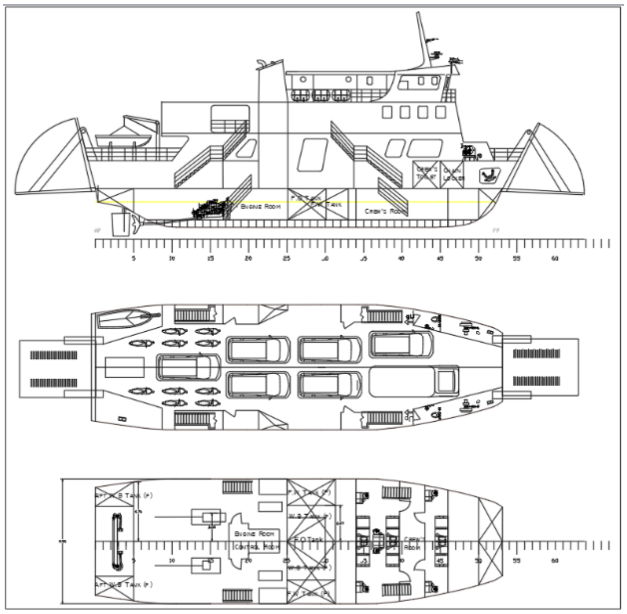

Figure 3. Model-3

The model is developed to analyze the hull form of the ship, so that the performance of each model can be compared to determine which one has the best stability. The following is data for the three ship models that will be analyzed.

Table 2. Principal Dimension of Ships Model

Dimension	Model-1	Model-2	Model-3
Length (m)	42,3	37	32
Breadth (m)	11,8	10,2	9,9
Height (m)	3,1	3,1	3,1
Draft (m)	2,03	2,03	2,03
Payload (Ton)	78,25	59,45	24,45

Vol.20 No.01, June 2026: page: 47-55
p - ISSN: 1978-886X
e - ISSN: 2614-641X

In the context of stability analysis, which refers to the vessel's ability to return to its original position after being subjected to external forces, the primary factor influencing stability is the dynamic righting arm (GZ), which generates a couple moment to balance the forces of buoyancy and gravity. The elements of stability include GZ, KG, and GM. Determining the value of the dynamic righting arm (GZ) is a crucial aspect in the evaluation of ship stability. Once the GZ value is obtained, the results are verified using the "Intact Stability Code" standard from the IMO (Ariany et al., 2022).

The results of the ship stability analysis under various loading percentage conditions are presented in Table 2.

Table 3. The Percentage of Loadcase

The Condition	Loadcase Percentage			
	1	2	3	4
Fuel oil	100%	50%	10%	0%
Cargo load	100%	100%	100%	0%
Water ballast	0%	0%	0%	0%
Fresh water	50%	10%	0%	0%

Based on the loadcase data provided, scenarios 2 and 3 represent intermediate conditions where fuel oil and freshwater levels are significantly reduced (50% to 10%) while maintaining a full cargo load. This typically leads to a rise in the vessel's vertical center of gravity (KG), potentially compromising the metacentric height (GM).

In the context of stability based on IMO criteria, ships with lower VCG and lighter payloads increasingly meet stringent stability requirements due to improved GM values and GZ area. Changes in VCG resulting from variations in payload and fuel must be considered in the stability analysis to ensure that the vessel remains safe under various operational conditions as defined by the loadcase. The stability of the Ro-Ro ferry operating on the Bengkalis–Sungai Pakning route refers to the following design criteria applicable to all ships (RESOLUTION MSC 267(85), 2008).

Table 4. IMO Criteria of Stability

Criteria	Value	Units
Max GZ Area 0 to 30	3,151	m.deg
Max GZ Area 0 to 40	5,157	m.deg
Max GZ Area 30 to 40	1,719	m.deg
Angle of Max GZ at 30 or greater	0,2	m
3.1.2.3: Angle of maximum GZ	25	deg
Initial GMt	0,15	m

Based on the results of the stability analysis of the three Ro-Ro ferry models with different payloads, varying stability values were obtained. All three ship models meet the IMO stability criteria. Nevertheless, Model-1 exhibits the best stability under all loadcase conditions, as it consistently demonstrates the highest values in the main stability parameters: the maximum GZ value, the ideal angle of maximum GZ, and the largest initial GMT (metacentric height) in every loading and fuel scenario. The rolling period of a ship is influenced by variations in the value of the metacentric height (Mukti et al., 2024).

Table 5. Lack of Input Data

Item	Model-1	Model-2	Model-3
Displacement (Ton)	730,9	549,9	463,8
WPA (m^2)	328,508	222,386	171,895
Inertia WPA (I_t) (m^4)	1,85	1,28	1,02
KB (m)	1,095	1,093	1,09
BM (m)	3,651	3,478	3,302
KG fluid (m)	2,8	2,65	2,55

The area under the GZ curve (m·deg) represents the ship's stability energy, where a larger area indicates that the vessel is more resistant to capsizing and more easily returns to an upright or stable position (Belenky et al., 2011). Regarding the maximum GZ value and its corresponding angle, their attainment reflects the vessel's ability to resist heeling in wave conditions; the greater the value and the closer the angle is to the optimal range (above 25°), the safer the vessel becomes. As for the initial GMT, a higher initial GMT value (above the minimum requirement of 0.15 m) indicates better initial stability of the vessel against rolling and load shifting.

Table 6. The GZ (m) for Model-1

Heel to Starboard (deg)	Every Condition of GZ (m)			
	1	2	3	4
0	0	0	0	0
10	0,74	0,81	0,855	0,868
20	0,931	1,069	1,172	1,204
30	0,929	1,081	1,191	1,227
40	0,837	0,98	1,077	1,113
50	0,691	0,814	0,893	0,927
60	0,51	0,608	0,665	0,695
70	0,307	0,377	0,41	0,436
80	0,091	0,131	0,139	0,159
90	-0,128	-0,121	-0,139	-0,125

In all four conditions, the maximum righting lever occurs at approximately 30^0 of heel. For Condition-4, GZ_{max} reaches 1.227 m. This suggests a robust restorative capability against capsizing moments at moderate angles.

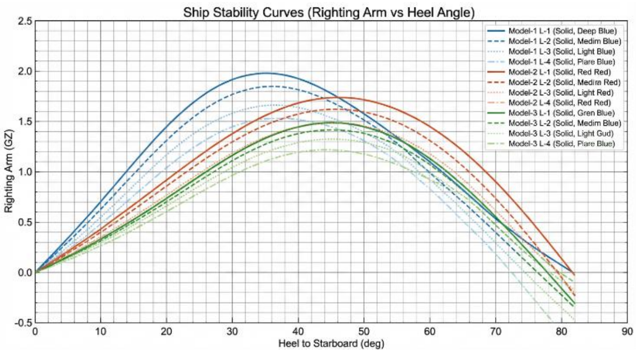

Figure 4. Ship Stability Curves

Figure 4 illustrates the stability curves for all models and loadcases in accordance with the specifications outlined in Table 7.

Table 7. Data input every model and loadcase

Name of Model and Loadcase's Number	Explanation
Model-1 Loadcase-1 (L-1)	3.1.2.4: Initial GMT GM at 0,0 deg = 4,856 m Max GZ= 0,94 m at 25.5 deg.
Model-1 Loadcase-2 (L-2)	3.1.2.4: Initial GMT GM at 0,0 deg = 4,999 m Max GZ= 1,092 m at 25.5 deg.
Model-1 Loadcase-3 (L3)	3.1.2.4: Initial GMT GM at 0,0 deg = 5,099 m Max GZ= 1,204 m at 25.5 deg.
Model-1 Loadcase-4 (L4)	3.1.2.4: Initial GMT GM at 0,0 deg = 5,145 m Max GZ= 1,24 m at 26,4 deg.
Model-2 Loadcase-1 (L-1)	3.1.2.4: Initial GMT GM at 0,0 deg = 2,693 m Max GZ= 0,562 m at 27,3 deg.
Model-2 Loadcase-2 (L-2)	3.1.2.4: Initial GMT GM at 0,0 deg = 3,327 m Max GZ= 0,768 m at 28,2 deg.
Model-2 Loadcase-3 (L-3)	3.1.2.4: Initial GMT GM at 0,0 deg = 3,567 m Max GZ= 0,903 m at 28,2 deg.
Model-2 Loadcase-4 (L-4)	3.1.2.4: Initial GMT GM at 0,0 deg = 3,636 m Max GZ= 0,95 m at 28,2 deg.
Model-3 Loadcase-1 (L-1)	3.1.2.4: Initial GMT GM at 0,0 deg = 3,341 m Max GZ= 0,87 m at 29,1 deg.
Model-3 Loadcase-2 (L-2)	3.1.2.4: Initial GMT GM at 0,0 deg = 3,488 m Max GZ= 1,027 m at 30 deg.
Model-3 Loadcase-3 (L-3)	3.1.2.4: Initial GMT GM at 0,0 deg = 3,596 m Max GZ= 1,137 m at 30 deg.
Model-3 Loadcase-4 (L-4)	3.1.2.4: Initial GMT GM at 0,0 deg = 3,655 m Max GZ= 1,18 m at 30,9 deg.

According to figure 4, The vessel maintains positive stability up to 80^0. However, at 90^0 the GZ values turn negative 0.125 m in Condition-4, indicating that the angle of vanishing stability occurs between 80^0 and 90^0. The steep increase in GZ values between 0^0 and 10^0 indicates a high Metacentric Height (GM), which is typical for wide beamed vessels like Ro-Ro ferries (B = 11.8 m relative to T = 2.03 m).

Table 8. The GZ (m) for Model-2

Heel to Starboard (deg)	Every Condition of GZ (m)			
	1	2	3	4
0	0	0	0	0
10	0,378	0,491	0,555	0,574

Wave: Jurnal Ilmiah Teknologi Maritim **Vol.20 No.01, June 2026: page: 47-55**
(Journal of Maritime Technology) p - ISSN: 1978-886X
e - ISSN: 2614-641X

20	0,538	0,724	0,845	0,883
30	0,558	0,766	0,901	0,949
40	0,502	0,704	0,829	0,878
50	0,406	0,587	0,693	0,74
60	0,29	0,44	0,519	0,563
70	0,165	0,277	0,325	0,362
80	0,036	0,104	0,119	0,149
90	-0,091	-0,072	-0,092	-0,069

The vessel maintains a positive righting lever up to 80^0. However, a transition to negative stability occurs at 90^0 (ranging from −0.069 to −0.092 m), indicating that the angle of vanishing stability lies between 80^0 and 90^0. The initial stability performance, there is a significant increase in GZ values within the 0^0 to 20^0 range, which suggests a high initial Metacentric Height.

Table 8. The GZ (m) for Model-3

Heel to Starboard (deg)	Every Condition of GZ (m)			
	1	2	3	4
0	0	0	0	0
10	0,573	0,61	0,631	0,641
20	0,819	0,946	1,035	1,066
30	0,87	1,027	1,137	1,18
40	0,828	0,985	1,089	1,134
50	0,726	0,867	0,953	0,997
60	0,584	0,7	0,764	0,805
70	0,415	0,503	0,541	0,578
80	0,229	0,285	0,297	0,329
90	0,034	0,057	0,042	0,068

In the first dataset, GZmax occurs at 300 with values reaching up to 0.949 m. In the second dataset, GZmax also peaks at 300, but with significantly higher values up to 1.18 m. The vessel exhibits positive stability up to 800 (0.149 m), but stability becomes negative at 900 (-0.069 m), indicating the angle of vanishing stability is between 800 and 900.

The vessel maintains positive stability through the entire 900 range, with a GZ of 0.068 m at the final measurement. Both sets show a rapid increase in GZ from 00 to 100 (reaching up to 0.641 m), which signifies a high Metacentric Height (GM).

The stability according to IMO criteria, ships with a lower vertical center of gravity (VCG) and lighter payload are more likely to meet stringent stability requirements due to higher GM values and larger GZ areas. Variations in VCG resulting from changes in payload and fuel must be considered in the stability analysis to ensure that the vessel remains safe under various operational conditions as defined by the load cases.

$$KG\ baru = \frac{(WxKG) + (w1xVCG1) + (w2xVCG2) + \dots}{W + w1 + w2 + \dots}$$

W : Initial displacement of the ship (ton)
KG : initial center of gravity height (m)
wi : Load weight i (ton)
VCGi : Vertical center of gravity of load i from the keel (m)

This process is repeated for each payload and loading/fuel scenario in the given load cases. Changes in the vertical center of gravity (KG) can be quantitatively calculated using the summation of weights and moments for each loading and fuel condition. The KG will increase if the cargo or fuel has a high VCG and decrease if the cargo is positioned below the initial KG of the vessel. This is essential for determining the ship's stability in every load case. The curve displays four loading conditions (L-1 to L-4) for each model, with Model-1 curves rendered in blue, Model-2 in red, and Model-3 in green.

Model-1 exhibits the highest maximum righting arm (GZ), reaching approximately 2.0 meters at a heel angle of around 40–45 degrees. The area under the GZ curve, which represents the ship's ability to recover from heeling, is also the largest among the three models. The GZ curve for Model-1 remains positive up to large heel angles (>80 degrees), indicating superior stability under various loading conditions. Model-2 demonstrates a slightly lower maximum GZ value, approximately 1.7–1.8 meters at a similar heel angle. The area under the curve is smaller than that of Model-1 but still indicates adequate stability. The GZ curve remains positive up to large heel angles, fulfilling the basic stability requirements. Model-3 shows the lowest maximum GZ, approximately 1.4–1.5 meters, and the smallest area under the curve. Although the GZ curve remains positive, the overall stability is lower compared to the other models. The fundamental design process is categorized into two distinct stages, the conceptual phase and the preliminary design (Cepowski & Chorab, 2021).

Compliance with IMO stability standards and national regulatory frameworks is paramount for maritime safety. Under the requirements of the Albanian Register of Shipping, vessels must undergo stability assessments, documenting the results in an amended stability booklet to maintain certification after modifications. Although diverse methodologies exist for determining approximate ship dimensions with acceptable reliability, these tools serve as preliminary estimates. Consequently, their usage remains limited until verified by definitive stability calculations (Lapa, 2020).

This process is repeated for each payload and loading/fuel scenario in the given load cases. Changes in the vertical center of gravity (KG) can be quantitatively calculated using the summation of weights and moments for each loading and fuel condition. The KG will increase if the cargo or fuel has a high VCG and decrease if the cargo is positioned below the initial KG of the vessel. This is essential for determining the ship's stability in every load case.

CONCLUSION

Based on the analysis, Model-1 satisfies the IMO stability criteria most effectively, as it possesses the highest maximum righting arm, the largest area under the curve, and an appropriate heel angle for maximum GZ. Therefore, Model-1 demonstrates the best stability performance among the three models. Among the designs, Model-3 demonstrates the lowest maximum GZ (approx. 1.4–1.5 m) and the smallest integral area under the curve. Despite maintaining a positive GZ range, its total stability is significantly reduced relative to the alternative models.

REFERENCE

Ariany, Z., Ariany, Z., Santoso, B., Sarwoko, & Prasetyo, N. A. (2022). Damage Stability Study of A 500 DW Ro-Ro Ferry Vessel Damage Stability Study of A 500 DW Ro-Ro Ferry Vessel. *Makara Journal of Technology*, *26*(3). https://doi.org/10.7454/mst.v26i3.1440.

Ariesta, R. C., Aliffrananda, M. H. N., Riyadi, S., & Utama, I. K. A. P. (2021). An Investigation into the Justification of the Service Speed of Ro-Ro Ferry with Block Coefficient 0 . 8 Based on the Resistance and Seakeeping Performance. *ICSOT Indonesia*, *November*, 19–20.

Awwalin, R., Marsudi, S., & Khusniawati, F. (2022). DESAIN KONSEPTUAL PERENCANAAN TRANSPORTASI LAUT WATERBUS ,. *Wave*, *16*, 51–58.

Belenky, V., Bassler, C. C., & Spyrou, K. J. (2011). *Development of Second Generation Intact Stability Criteria* (Issue December).

Cepowski, T., & Chorab, P. (2021). Determination of design formulas for container ships at the preliminary design stage using artificial neural network and multiple nonlinear regression. *Ocean Engineering*, *238*(July). https://doi.org/10.1016/j.oceaneng.2021.109727.

Dewanto, C. C., & Nasirudin, A. (2023). SHIP LIGHTWEIGHT ESTIMATION AT CONCEPT DESIGN STAGE : CASE OF INDONESIA SINGLE ENDED RO-RO FERRIES. *Journal of Marine-Earth Science Technology*, *3*(3), 86–89. https://doi.org/10.12962/j27745449.v3i3.697.

Lapa, K. (2020). Assessment of the Stability of Passenger Ships in Coastal Navigation in Cas of Lacking Ship Geometry Data. *Transactions on Maritime Science*, *02*, 150–160. https://doi.org/doi.10.7225/toms.v09.n02.002.

Mukti, H. P., Chrismianto, D., & Manik, P. (2024). Analisa Stabilitas Kapal General Cargo 11280 DWT Dengan Rute Pelayaran Surabaya - Makassar. *Teknik Perkapalan*, *12*(4), 1–9.

Perhubungan, R. M. (2016). *Peraturan Menteri Perhubungan Republik Indonesia Nomor PM 30 Tahun 2016* (p. 7). https://jdih.maritim.go.id/cfind/source/files/permenhub/2016/permenhub_pm_30_tahun_2016.pdf.

Projektovanja, I. I., Privredu, Z. A., & Prabowo, A. R. (2022). Performance evaluation on the designed v-shaped monohull ship models. *Journal of Applied Engineering Science*, *20*, 610–624. https://doi.org/10.5937/jaes0-35481.

Rawson, K.J; Tupper, E. . (2001). Basic Ship Theory. In *Basic Ship Theory* (5th Editio). Butterworth Heinemann. https://doi.org/10.1016/b978-0-7506-5398-5.x5000-6.

RESOLUTION MSC 267(85), 267 (2008).

Skoupas, S., Zaraphonitis, G., & Papanikolaou, A. (2019). Parametric design and optimisation of high-speed Ro-Ro Passenger ships. *Ocean Engineering*, *189*(August), 106346.

Szymo, M. (2024). Safety Management on Ro-Ro Passenger Ships. *TRANSNAV the International Journal on Marine Navigation and Safety of Sea Transportation*, *18*(2), 281–285. https://doi.org/10.12716/1001.18.02.02.